INSTITUTE OF PHYSICS PUBLISHING JOURNAL OF PHYSICS D: APPLIED PHYSICS

J. Phys. D: Appl. Phys. **39** (2006) 1739–1742 doi:10.1088/0022-3727/39/9/005

Local study of the magnetism of Co-doped ZnO thin films

M S Moreno[1,2], T Kasama[1,3], R E Dunin-Borkowski[1,3], D Cooper[1], P A Midgley[1], L B Steren[2], S Duhalde[4] and M F Vignolo[4]

[1] Department of Materials Science and Metallurgy, University of Cambridge, Pembroke Street, Cambridge CB2 3QZ, UK
[2] Centro Atómico Bariloche and Instituto Balseiro, 8400 San Carlos de Bariloche, Argentina
[3] Frontier Research System, Institute of Physical and Chemical Research, Hatoyama, Saitama 350-0395, Japan
[4] Laboratorio de Ablación Láser, Facultad de Ingeniería, Universidad de Buenos Aires, Paseo Colón 850, 1063 Buenos Aires, Argentina

Received 25 October 2005
Published 20 April 2006
Online at stacks.iop.org/JPhysD/39/1739

Abstract
Complementary electron microscopy techniques that provide local information about structural, electronic and magnetic properties have been used to study thin films of $Zn_{0.85}Co_{0.15}O$ grown on Si_3N_4 buffered (100) Si substrates at 673 K. No evidence of secondary phases at interfaces was found. For this growth temperature, Co is incorporated into the ZnO lattice by substituting for Zn, and its oxidation state is 2^+. Off-axis electron holography reveals no measurable magnetic signal, either at domains or at interfaces, in agreement with macroscopic measurements that indicate a non-ferromagnetic behaviour.

1. Introduction

Dilute magnetic semiconductors (DMS), which are formed by incorporating magnetic impurities into semiconductors, have attracted much interest due to their possible applications in spintronic devices. However, the development of practical thin film and spintronic devices that operate at ambient conditions relies on a full understanding of their magnetic properties in this high temperature regime. Among the candidate materials for such applications, some of the most widely studied so far are thin films of ZnO doped with different transition metal elements (TM). For doping with Co, the absence of ferromagnetism has been reported in polycrystalline materials [1–5]. Controversial results from thin films include a report of spin-glass behaviour [6], whereas theoretical work has indicated that a ferromagnetic state should be more stable [7]. Confirmation of the existence of ferromagnetic order in ZnO : Co requires further investigation [8]. Ferromagnetism observed in thin films at room temperature has been explained either as an intrinsic property of the material [9–15] or in terms of the existence of segregated Co [16, 17]. Coey *et al* [18] suggested the presence of a spin–split donor impurity band with crystal defects in the interface region contributing to the stabilization of a spin triplet as the ground state [19]. Different substrate orientations have been used in these studies, including sapphire, Si and SiO_2/Si. For sapphire, Kim *et al* [16] reported homogeneous doping for deposition temperatures in the range 673–873 K and Co segregation at higher temperatures.

Based on the available literature, magnetic ordering in doped ZnO appears to depend strongly on the growth conditions used, which may in turn determine the presence of defects such as zinc and oxygen vacancies and zinc interstitials. Most experimental studies have been performed using macroscopic techniques to characterize the magnetic properties of such materials. Here we examine the local structural, electronic and magnetic properties of ZnO:Co thin films that have been grown on a substrate that provides a poorer lattice matching.

2. Experimental procedure

$Zn_{0.85}Co_{0.15}O$ thin films were grown on Si_3N_4-buffered (100) Si substrates by pulsed-laser deposition. An Nd : YAG laser, operating at 266 nm and 10 Hz, was focused on the target with an energy density of 3 J cm^{-2}. Thin films, 60–100 nm in thickness, were deposited at 673 K and 4 Pa background pressure in either argon or oxygen atmospheres during the deposition and cooling of the samples to room temperature. Local information from different areas of the

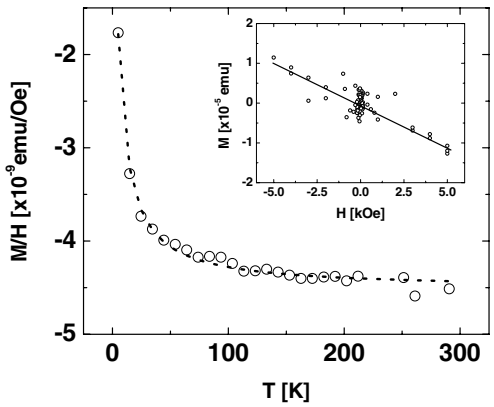

Figure 1. Temperature dependence of the magnetization, measured at 10 kOe. Inset: M versus H plot, measured at 35 K in the same sample. Circles: experimental data. The solid line is a guide to the eye.

films was provided by using advanced transmission electron microscopy (TEM) techniques including high-resolution TEM, chemical mapping, electron energy-loss spectroscopy (EELS) and off-axis electron holography. This information was obtained at room temperature using a Tecnai F20 microscope equipped with a Gatan Imaging Filter (GIF) 2002 and a Philips CM300-ST microscope equipped with a Lorentz lens, an electrostatic biprism and a GIF 2000. Magnetic measurements were performed using a Quantum Design SQUID magnetometer at temperatures between 5 and 300 K and in magnetic fields of up to 50 kOe.

3. Results and discussion

The microstructure and properties of the films were found to be independent of the atmosphere used during deposition. For simplicity, we show here results obtained from the film deposited in an Ar atmosphere. The temperature dependence of the magnetization in this film is shown in figure 1. The curve is fitted by the sum of a diamagnetic contribution, arising primarily from the film substrate and the ZnO matrix and a Curie–Weiss paramagnetic component of the Co ions. The magnetization versus field curve, measured for the same sample at $T = 35$ K, is plotted in the inset figure. The magnetization varies linearly with the applied magnetic field. The negative slope indicates that the diamagnetic contribution is larger than the paramagnetic contribution at this temperature. All the samples examined presented similar magnetization behaviour. None presented signatures of ferromagnetism in these measurements.

Electron diffraction revealed only reflections corresponding to the wurzite structure of ZnO, with highly textured growth along the 0001 axis. Electron diffraction patterns (figure 2(*a*)), recorded from regions at least 0.5 μm in size, revealed continuous intensity distributions resulting from the presence of nanometre-sized structural domains. The anisotropic angular intensity distribution visible in figure 2(*a*) results from the presence of a high degree of in-plane texture. Special attention was paid to these rotated domains and to interfaces between them as potential sources of chemical, electronic and magnetic anomalies. Electron diffraction patterns and high-resolution images

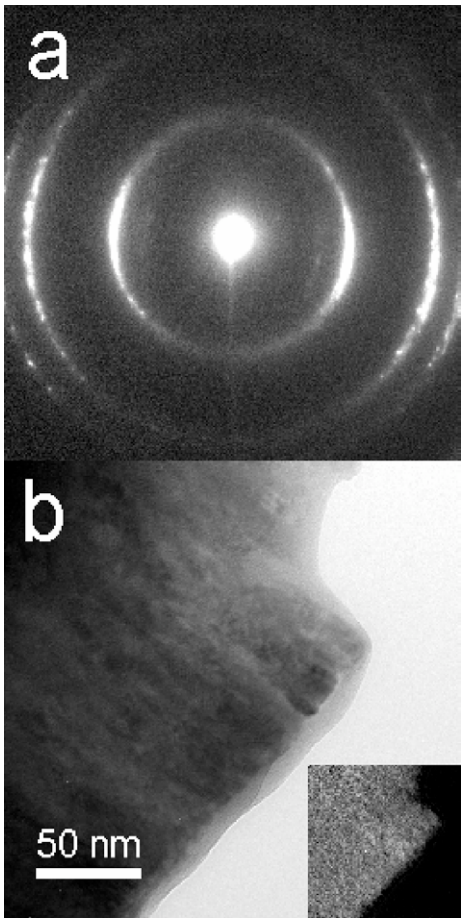

Figure 2. (*a*) Electron diffraction pattern acquired from the $Zn_{0.85}Co_{0.15}O$ film. The rings correspond to the (100), (110) and (200) reflexions. (*b*) Bright-field TEM image. Inset: map of Co distribution in the same region.

did not reveal the presence of secondary phases, and chemical mapping for Co, shown in the inset of figure 2(*b*), showed a uniform distribution of Co across the sample.

The oxidation state of Co in the films was determined using EELS. Spectra were acquired from different nanometre-sized regions, including domain boundaries and individual grains, and analysed using standard techniques [20]. Figure 3 (upper panel) shows a spectrum that contains the Co $L_{2,3}$ and the O K edges. The Co L_3 and L_2 edges did not vary in intensity or position between the different points analysed. The lack of a change in the ratio of the intensities of the white lines indicates that the oxidation state of Co does not change across the films. A comparison of these spectra with reference materials [21,22] is shown in figure 3(lower panel). Note the similarity between the spectrum of our doped ZnO and that of CoO. It strongly indicates that the oxidation state of Co is 2+, in agreement with the results of other techniques, which suggests that Co substitutes for Zn in the lattice uniformly. We also note the different line widths of Co_3O_4 and our doped ZnO, due to the two oxidation states of Co, 2+ and 3+, in the spinel. This reinforces our conclusion that the Co ions are substituting for Zn. The comparison with the spectrum of Co_3O_4 in terms of intensities is not so straightforward as with CoO because of the different contributions of the continuous background. The background can be eliminated using different methods [23].

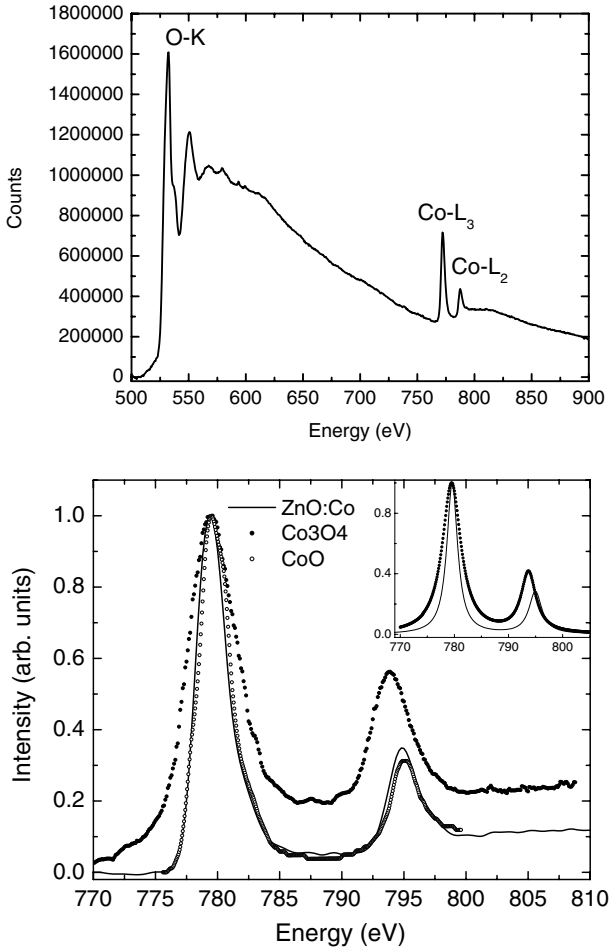

Figure 3. Background subtracted EELS spectrum (upper panel). Comparison of the $L_{2,3}$ Co edge of the doped ZnO and the reference materials CoO [21] and Co_3O_4 [22]. In the inset are compared the background subtracted spectra of our doped ZnO and Co_3O_4.

We have used a standard fitting procedure [24], that uses model functions for the background and Lorentz functions for the white lines. After fitting, a background subtracted spectra can be obtained and compared as shown in the inset of figure 3 (lower panel) for Co_3O_4 and our doped ZnO. The different intensities can be now appreciated more clearly, making more evident the different valences. The oxygen edge presents a fine structure consisting of one peak within the first 10 eV above threshold. This fine structure is different from that of oxygen in CoO [21], which presents two strong peaks within that energy range, and very similar to that of oxygen in ZnO [25].

Off-axis electron holography in the TEM was used to image the remanent magnetic states of the films at room temperature. This technique allows the phase shift of a high-energy electron wave that has passed through a specimen to be recorded [26]. The phase shift ϕ can be used to measure electrostatic and magnetic fields with nanometre spatial resolution. The magnetic contribution to the phase shift is given by the expression

$$\phi_{\mathrm{MAG}}(x) = -\left(\frac{e}{\hbar}\right)\iint B_{\perp}(x, z)\,\mathrm{d}x\,\mathrm{d}z, \qquad (1)$$

where z is the incident electron beam direction, x is a direction in the plane of the specimen and $B_{\perp}$ is the component of the magnetic induction perpendicular to both x and z. The gradient of the magnetic contribution to the phase shift can be used to image the magnitude distribution of in-plane magnetic component.

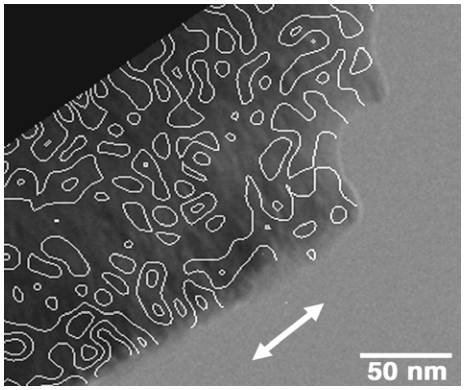

Figure 4. Magnetic induction map of a remanent state measured using electron holography, superimposed onto a bright-field image. The contour spacing is 0.049 rad. The sample was saturated magnetically in the direction of the arrow before removing the applied field and recording the hologram. The mean inner potential contribution to the phase shift has been subtracted from the measurements before forming the contour map.

Off-axis electron holograms were acquired at 300 kV using a Lorentz minilens, with the conventional microscope objective lens switched off and the sample located in magnetic-field-free conditions. Reference holograms from a vacuum were acquired to remove distortions associated with the imaging and recording system of the microscope. Samples were saturated magnetically parallel to the sample edge by using the field of the objective lens to apply in-plane fields of ~10 000 Oe with the sample tilted at ±30°. The sample was always tilted back to 0° in zero field and imaged at remanence.

Figure 4 shows contours generated directly from the magnetic contribution to the measured holographic phase shift, after subtracting the mean inner potential contribution from each recorded phase image, using a procedure that is described in detail elsewhere [26]. The contour spacing of 0.049 rad, which is equal to an enclosed magnetic flux of 3.125×10^{-17} Wb between adjacent contours, is inversely proportional to the in-plane component of the magnetic induction in the sample integrated in the electron beam direction. Only noise is visible in figure 3, indicating that there is no measurable local magnetic signal either in the domains or at boundaries between them. Similar results were obtained from the two samples examined. An upper limit to the measured in-plane magnetic induction measured in figure 4 is ~0.003 T, on the assumption that Co distributes uniformly across the field of view and that all the magnetic moments align within the plane of the sample. These observations also suggest that Co has not segregated in the samples.

4. Conclusions

In summary, we have produced thin films of $Zn_{0.85}Co_{0.15}O$ in different atmospheres. Advanced TEM techniques have been

used to provide local information about the microstructural, chemical, electronic and magnetic properties of the films. The combination of these techniques suggests strongly that Co replaces Zn substitutionally in the ZnO lattice and that at a local level the Co-doped ZnO thin films are non-magnetic at room temperature. The observed properties are independent of the atmosphere used during deposition.

Acknowledgments

This work was partially supported by FundaciónAntorchas, FONCyT (PICT 13297) and CONICET, (Argentina). MSM and RDB thank the Royal Society for financial support.

References

[1] Lawes G, Risbud A, Ramirez A P and Seshadri R 2005 *Phys. Rev.* B **71** 045201
[2] Kolesnik S, Danrowski B and Mais J 2005 *J. Appl. Phys.* **95** 2582
[3] Bouloudenine M, Viart N, Colis S, Kortus J and Dinia A 2005 *Appl. Phys. Lett.* **87** 052501
[4] Kane M H, Shalini K, Summers C J, Varatharajan R, Nause J, Vestal C, Zhang Z and Ferguson I 2005 *J. Appl. Phys.* **97** 023906
[5] Yoon S W, Cho S -B, We S, Yoon S, Suh B, Song H and Shin Y J 2003 *J. Appl. Phys.* **93** 7879
[6] Fukumura T, Jin Z, Kawasaki M, Shono T, Hasegawa T, Koshibara S and Koinuma H 2001 *Appl. Phys. Lett.* **78** 958
[7] Sato K and Katayama-Yoshida H 2001 *Physica* B **308–310** 904–7
[8] Sluiter M, Kawazoe Y, Sharma P, Inoue A, Raju A, Rout C and Waghmare U 2005 *Phys. Rev. Lett.* **94** 187204 and references therein
[9] Ramachandran S, Tiwari A and Narayan J 2004 *Appl. Phys. Lett.* **84** 5255
[10] Lee H-J, Jeong S -Y, Cho C R and Park C H 2002 *Appl. Phys. Lett.* **81** 4020
[11] Ueda K, Tabata H and Kawai T 2001 *Appl. Phys. Lett.* **79** 988
[12] Dorneles L S, O'Mahony D, Fitzgerald C B, McGee F, Venkatesan M, Stanca I, Lunney J G and Coey J M D 2005 *Appl. Surf. Sci.* **248** 406
[13] Yin Z, Chen N, Chai C and Yang F 2004 *J. Appl. Phys.* **96** 5093
[14] Dinia A, Schmerber G, Mény C, Pierron-Bohnes V and Beaurepaire E 2005 *J. Appl. Phys.* **97** 123908
[15] Yan L, Ong C K and Rao X S 2004 *J. Appl. Phys.* **96** 508
[16] Kim J H, Kim H, Kim D, Ihm Y and Choo W K 2004 *J. Eur. Ceram. Soc.* **24** 1847
[17] Park J H, Kim M G, Jang H M, Ryu S and Kim Y M, 2004 *Appl. Phys. Lett.* **84** 1338
[18] Coey J M D, Venkatesan M and Fitzgerald C B 2005 *Nat. Mater.* **4** 173
[19] Coey J M D 2005 *J. Appl. Phys.* **97** 10D313
[20] Egerton R F 1996 *Electron Energy-Loss Spectroscopy in the Electron Microscope* (New York: Plenum)
[21] Mitterbauer C *et al* 2003 *Ultramicroscopy* **96** 469
[22] Wang Z L and Yin J S 1998 *Phil. Mag.* B **77** 49
[23] Riedl T, Gemming T and Wetzig K 2006 *Ultramicroscopy* **106** 284
[24] Wang F, Malac M and Egerton R F 2006 *Micron* at press
[25] Giannakopoulos K, Boukos N and Travlos A 2006 *Superlatt. Microstruct.* **39** 115
[26] Dunin-Borkowski R E, McCartney M R and Smith D J 2004 *Encyclopedia of Nanoscience and Nanotechnology* vol 3, ed H S Nalwa (California: American Scientific Publishers) pp 41–100